ISSN 1023-1935, Russian Journal of Electrochemistry, 2017, Vol. 53, No. 5, pp. 509–521. © Pleiades Publishing, Ltd., 2017.
Original Russian Text © V.V. Yanilkin, N.V. Nastapova, G.R. Nasretdinova, R.R. Fazleeva, S.V. Fedorenko, A.R. Mustafina, Yu.N. Osin, 2017, published in Elektrokhimiya, 2017, Vol. 53, No. 5, pp. 578–591.

Methylviologen-Mediated Electrochemical Synthesis of Platinum Nanoparticles in Solution Bulk

V. V. Yanilkin[a], *, N. V. Nastapova[a], G. R. Nasretdinova[a], R. R. Fazleeva[a], S. V. Fedorenko[a], A. R. Mustafina[a], and Yu. N. Osin[b]

[a] *Arbuzov Institute of Organic and Physical Chemistry, Kazan Research Center, Russian Academy of Sciences, Kazan, 420088 Russia*

[b] *Kazan (Volga region) Federal University, Interdisciplinary Center "Analytical Microscopy," Kazan, 420018 Russia*

**e-mail: yanilkin@iopc.ru*

Received May 18, 2016

Abstract—Platinum nanoparticles (PtNPs) are synthesized by methylviologen-mediated reduction of $PtCl_2$ at the potentials of the $MV^{2+}/MV^{\bullet+}$ redox couple in 40% aqueous DMF solution. In the absence of stabilizing agents and in the presence of a stabilizer in the form of spherical silica NPs or alkylamine-modified silica NPs (SiO_2-NHR), a part of PtNPs (14–18%) are deposited on the electrode while the rest of particles remain in solution to form coarse aggregates which precipitate. In the latter case, PtNPs are also partly bound to form individual ultrafine NPs (3 ± 2 nm) on the SiO_2-NHR surface. In the presence of polyvinylpyrrolidone (PVP), the generated PtNPs (18 ± 9 nm) neither aggregate nor deposit on the cathode but are completely stabilized in solution being encapsulated within the PVP matrix. The obtained PtNPs are characterized by the methods of dynamic light-scattering and electron microscopy.

Keywords: electrosynthesis, nanoparticles, platinum, mediator, methylviologen, polyvinylpyrrolidone, silica nanoparticles

DOI: 10.1134/S1023193517050160

INTRODUCTION

In the recent years, attention was focused on metal nanoparticles (MNPs) due to their unusual properties and the wide diversity of their possible applications in catalysis, electronics, biomedicine, optics, analysis, etc. [1–7]. MNPs are known for a long time, for instance, AuNPs (colloid gold) were first synthesized by Faraday back in 1857 [8]. Their active study started relatively recently, only 20–25 years ago. First, the physical methods of MNPs preparation based on evaporation of the bulk metal by one or another physical procedure followed by condensation of atoms to form NPs were considered to be most promising. However, at present the most successful and widely used method of their synthesis is the chemical reduction of metal ions and complexes in solution under the action of various reducers. Biochemical methods have found limited application in the synthesis of MNPs; there are only few examples of such synthesis of NPs of gold, silver, copper, and zinc [9, 10].

The electrochemical method is commonly used in synthesizing MNPs immobilized on a conducting support (electrode). Various versions of this method were recently analyzed by Petrii in his through review [11]. However, the electrochemical methods of synthesizing MNPs in their different states (in solution volume, on nonconducting solid supports, in matrices, in nanocapsules, etc.) are not yet so well developed.

Dispersion of bulk metal electrodes during their electrolysis was among the first methods of electrochemical synthesis of colloid metals in solution. This phenomenon was first described by Haber [12] more than 100 years ago (see [11] and references therein). Dispersion of electrodes proceeds at high potentials under both dc and ac conditions and is accompanied by hydrogen evolution.

The other specially developed methods of MNPs synthesis under soft conditions are more attractive. They are based on selective electroreduction (ER) of metal ions (complexes). However, it is well known that the thus generated metal is deposited on the electrode surface, which forms the basis of the industrial processes for production of metals, metal blacks, electroplates, and also in refining of metals. In the presence of stabilizers of NPs, the fraction of deposited metal decreases, albeit remains high. Thus, at the synthesis of AgNPs in solution by ER of silver ions in the presence of polyvinylpyrrolidone (PVP), up to 80% of the metal is deposited on the cathode, while in the presence of salts of tetraalkylammonium R_4NX and sodium dodecylbenzenesulfonate $C_{12}H_{25}C_6H_4SO_3Na$, virtually

all generated metal is deposited on the electrode [13, 14]. This is why almost all methods of MNPs generation use the procedures that solve in one way or another the problem of metal deposition. For instance, to decrease the contribution of this process, it was proposed to combine the production of MNPs on the electrode surface during the short-term pulse electrolysis with the subsequent process of transfer of these particles to solution by supersonic treatment of the electrode (pulse sonoelectrochemistry) [15–17].

Reetz et all [18–22] proposed another method for MNPs electrosynthesis. This is the diaphragmless electrolysis in aprotic organic media (tetrahydrofuran, dimethylformamide (DMF), acetonitrile or their mixtures) which employs a dissolving anode, a platinum cathode, and also salts of tetraalkylammonium R_4N^+ or teteraalkylphosphonium R_4P^+ (R is a long alkyl radical) as the supporting electrolyte. The proposed scheme of this process involves the following sequence of stages: anode dissolution to form metal ions, their diffusion to the cathode surface and reduction on this surface to form metal(0). It is assumed that surface-active ammonium and phosphonium cations should prevent the metal deposition on the electrode and stabilize MNPs in solution. Despite the simplicity of this method, its application is limited by the necessity of using only aprotic media and surface-active cations. Moreover, in the initial period of electrolysis when metal ions are absent in solution, the supporting electrolyte cations are reduced on the cathode instead of ions of the given metal. This side process occurs not only in the beginning but also during the electrolysis until a considerable concentration of metal ions capable of supporting the necessary electrolysis current is accumulated. This means that in the end of electrolysis, a certain concentration of ions of the given metal remains in solution. Furthermore, a part of metal inevitably deposit on the electrode [13, 14]. It is probable that, as a result of action of these factors, the yield of MNPs does not exceed 60% in many cases.

Recently [23–35], a method of mediated electrosynthesis of MNPs was proposed, which has several undeniable advantages and is an alternative to the aforementioned electrochemical methods of synthesis of NPs. Its distinguishing feature is that the process of metal ion reduction is transferred from the electrode surface to solution volume. In such process, on the cathode the reduced form the mediator is formed ($Med_{ox} + [e] \rightarrow Med_{red}$), which diffuses from the electrode surface to solution bulk where reduces the metal ions present there in one or another state (see above). When Med_{red} has a sufficient reducing power, a sort of "protective layer" is formed in the near-electrode layer, which intercepts the metal ions that arrive from solution bulk. Thus, with the aptly chosen mediator, both the metal reduction and its deposition on the electrode may be totally eliminated. The synthesis by this method requires no supersonic treatment used in pulse sonoelectrochemistry, is not confined to certain media and supporting electrolytes, and is not associated with any side processes typical of the Reetz method. The mediator method opens up a fundamentally new possibility of synthesizing MNPs in those cases where the reduction of the metal ion is complicated or impossible, e.g., for example, for insoluble or poorly soluble metal salts, for metal ions encapsulated in micelles, polymer globules, or other matrices, for their immobilization on a nonconducting solid support, and finally in the cases where the cathode and the metal salt are in different phases of a heterogeneous system.

The workability and efficiency of this method was demonstrated for synthesizing NPs of Pd [23–28], Ag [29–32], Co [33], Au [34, 35] in the absence and in the presence of stabilizers in aqueous, water-organic, and nonaqueus media, with the use of either metal salts or metal ions generated in situ in solution as a result of dissolution of the metal anode during the electrolysis. This method is equally efficient for soluble ions and complexes ($[PdCl_4]^{2-}$, Ag^+, AuCl, $[CoCl_4]^{2-}$) and insoluble metal salts (AgCl, spherical AgCl@CTAC nanoparticles (CTAC is cetyltrimethylammonium chloride), $[PdCl_4]^{2-}$@CTAC), irrespective of whether the mediator reduction proceeds more or less easily than the reduction of metal ion (complex). As the mediators, methylviologen [24–32, 34] and tetraviologen calix[4]resorcines were taken [23–26, 31, 32], as well as anthracene [33] and molecular oxygen [35]. The synthesized NPs were stabilized by tetraviologen calixresorcines themselves, by encapsulation in nanocapsules formed by polymeric spherical NPs, in PVP and CTAC shells, and also by binding to the surface of aminoalkylated silica NPs (SiO_2-NHR).

In this publication, we show the results of studying the possibility of using the mediated electrosynthesis for synthesizing PtNPs which are of interest first of all as the catalysts. So far, their electrochemical synthesis was carried out only by dispersing the platinum electrode [11, 36] and also by reducing $PtCl_2$ by the Reetz method [22].

EXPERIMENTAL

Our studies were carried out by the methods of cyclic voltammetry (CV), microelectrolysis, preparative electrolysis, scanning (SEM), transmission (TEM), and scanning transmission electron microscopy (STEM) and also dynamic light scattering (DLS).

Cyclic voltammograms (CV curves) were recorded by means of P-30J potentiostat (Elins, Russia) (without *IR* compensation) in argon atmosphere. A glassy carbon (GC) disc electrode (diameter 2.0 mm) sealed in glass served as the working electrode. Before each measurement, the electrode was cleaned by mechanical polishing. A Pt wire served as the counter elec-

trode. All potentials were measured and are shown with respect to the aqueous saturated calomel electrode (SCE) which had the potential of −0.41 V vs. E_0' (Fc^+/Fc) and was connected with the working solution by an electrolyte bridge filled with supporting electrolyte solution. In all voltammograms, the stationary potential served as the initial and the final potentials. The temperature was 295 K. The diffusion nature of peak current i_p was proved based on the theoretical shape of voltammograms and the linear dependence i_p vs. $v^{1/2}$ by varying the potential scan rate from 10 to 200 mV/s; its adsorption nature followed from the presence of the adsorption maximum.

The preparative electrolysis was carried out in a diaphragm (porous glass) three-electrode glass cell at the controlled potential of methylviologen reduction to radical cation (−0.80 V vs. SCE) by means of P-30J potentiostat in argon atmosphere at room temperature ($T = 295$ K). During the electrolysis, the solution was stirred with a magnetic stirrer. The working electrode was a glassy carbon plate; the reference electrode was SCE connected with the studied solution by a bridge filled with supporting electrolyte solution; the counter electrode represented a Pt wire immersed into supporting electrolyte solution. The electrolysis of solutions containing 1.5 mM $PtCl_2$, 2.0 mM $MV^{2+} \cdot 2PF_6^-$ and 0.1 M KPF_6 was carried out in the absence and in the presence of NPs stabilizer. The latter represented silica NPs (SiO_2, 2 g/L), SiO_2-NHR (1 g/L), and PVP (8.3 g/L). In the absence of stabilizer and in the presence of SiO_2, the solution volume and the electrode surface area were 10 mL and 4 cm^2, respectively. In the other cases, they were 15 mL and 5.6 cm^2, respectively. After the end of electrolysis, the resulting solution was studied by the CV method on the indicator GC electrode (diameter 2.0 mm) immediately in the cell.

NPs obtained in the course of electrolysis were precipitated by centrifuging (15000 rpm, 2 h), washed three times with water (in the presence of PVP, another procedure of NPs separation was used, as described below in the discussion of results), and dispersed in water by supersonic treatment. The resulting solution was studied by means of a complex of methods (SEM, TEM, STEM, and DLS). In the case of SEM, the solution was spread over the surface of titanium foil preliminarily cleaned of supersonication in water and acetone. Then the sample was dried in air at mild heating (to 40°C). For TEM and STEM, 10 μL of solution were placed on 3-mm copper grid with the formvar/carbon support and dried at room temperature. After complete drying, the grid was placed in the transmission electron microscope in a special graphite holder to carry out microanalysis.

Electron microscopic analysis. The morphology of the sample surface was studied on a high-resolution scanning electron microscope Merlin (Carl Zeiss, Germany) equipped with ASB, SE, and STEM detectors. The elemental analysis was carried out with the use of a detector of energy-dispersive spectrum AZTEC X-MAX (Oxford Instruments, UK) combined with the microscope. The TEM analysis of samples was carried out on a transmission electron microscope Hitachi HT7700 Excellence (Japan). The scanning was carried out at the accelerating voltage of 80 kV in the TEM mode; the elemental analysis was carried out in the STEM mode at the same parameters with the use of X-Max™ 80T (Oxford Instruments, UK). The maps of distribution of elements were plotted in the MAPS mode.

DLS measurements were carried out by means of the Zetasizer Nano device (Malvern Instruments, UK). The resulting autocorrelation functions were analyzed by using Malvern DTS programs.

The synthesis of water-soluble spherical silica NPs (SiO_2, 86 ± 25 nm) and alkylamine-modified silica NPs (SiO_2-NHR, 157 ± 40 nm) was carried out based on the use of 3-[2-(2-aminoethylamino)ethylamino]-propyltrimethoxysilane as the modifying agent according to the procedure described earlier [27]. Commercial reagents Na_2PtCl_4, $PtCl_2$, NaCl, KPF_6, poly(N-vinylpyrrolidone) (PVP, 40000 D), DMF, dimethylsulfoxide (DMSO) (Alfa Aesar), Bu_4NCl, Bu_4NBF_4 (Fluka), methylviologen (Acros), Bu_4NPF_6 (Aldrich) were used without additional cleaning. Twice distilled water was used.

RESULTS AND DISCUSSION

Platinum and palladium pertain to one and the same subgroup of platinum metals, and their properties are somewhat similar. In connection with this, at first we planned to carry out the mediated electrosynthesis of PtNPs in analogy with the mediated electrosynthesis of PdNPs in water-organic (DMF-H_2O) and nonaqueous (DMSO) media with the use of $[PtCl_4]^{2-}$ as the precursor and methylviologen as the mediator [24, 25]. However, it turned out that $[PtCl_4]^{2-}$ is reduced much more difficultly as compared with $[PdCl_4]^{2-}$. In aqueous and water-organic media [H_2O/0.1 M NaCl, and DMF (60 vol %)–H_2O/0.1 M NaCl (0.05 M Bu_4NCl)], this dianion is not reduced in the accessible potential region. In the nonaqueous medium DMSO/0.1 M Bu_4NCl, two irreversible reduction peaks are observed for $[PtCl_4]^{2-}$ (Fig. 1, curve *a*). The first peak is weakly pronounced and the second peak is predominant. For $PtCl_2$ under the analogous conditions with Bu_4NBF_4 or Bu_4NPF_6 as supporting salts, two peaks are also observed in the same potential region; however, in this case the first peak dominates (Fig. 2, curve *a*). In is obvious that in both cases, the first peak corresponds to the reduction

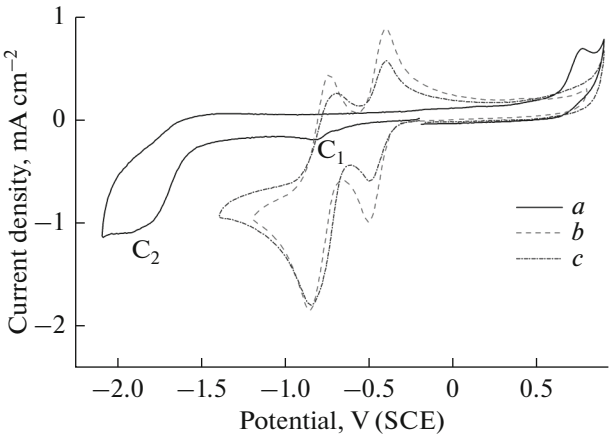

Fig. 1. CV curves in DMSO/0.1 M Bu_4NCl medium: (*a*) 1.5 mM Na_2PtCl_4; (*b*) 2.0 mM MV^{2+}; (*c*) 1.5 mM Na_2PtCl_4 and 2.0 mM MV^{2+}. v = 100 mV/s.

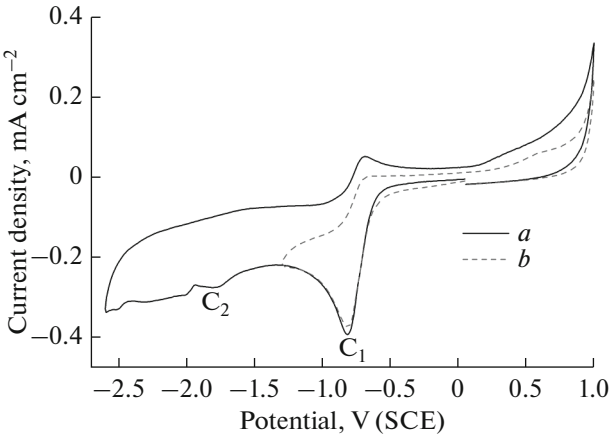

Fig. 2. CV curves of 1.5 mM $PtCl_2$ in DMSO/0.1 M Bu_4NPF_6. Reversal potential: (*a*) −2.60 V and (*b*) −1.30 V. v = 100 mV/s.

of $PtCl_2$ and the second peak pertains to the reduction of $[PtCl_4]^{2-}$ (Scheme 1).

$$PtCl_2 + 2e \xrightarrow{C_1} Pt^0 + 2Cl^-$$
$$PtCl_2 + 2Cl^- \rightleftharpoons [PtCl_4]^{2-}$$
$$[PtCl_4]^{2-} + 2e \xrightarrow{C_2} Pt^0 + 4Cl^-$$

Scheme 1. Scheme of reduction of $PtCl_2$ and $[PtCl_4]^{2-}$ in DMSO.

In solution, these species are in equilibrium and $[PtCl_4]^{2-}$ partially dissociates upon its introduction to solution to form $PtCl_2$. At the addition of $PtCl_2$ to solution, its reduction proceeds to form Pt^0 and chloride ions, the latter are bound with $PtCl_2$ to produce $[PtCl_4]^{2-}$. The reduction peaks of both species indicate that the equilibrium between them (Scheme 1) is established very slowly. Otherwise, the only reduction peak corresponding to the easily reducible form $PtCl_2$ should be observed. From the data obtained, it also follows that $[PtCl_4]^{2-}$ is reduced much more difficultly as compared with $[PdCl_4]^{2-}$ (ΔE_p = 0.95 V). Another difference of Pt from Pd [24–29] lies in the fact that the generated metal platinum is not dissolved anodically in the accessible potential range.

Methylviologen (MV^{2+}) is reduced in two steps with the transfer of one electron in each step to form the stable radical cation $MV^{\bullet+}$ and neutral diamine MV^0 (Scheme 2) [37]. In the first step, $[PtCl_4]^{2-}$ is reduced substantially easier (ΔE_p = 1.45 V); thus, upon the introduction of $[PtCl_4]^{2-}$ (from 0.5 to 3.0 mM), the height of its first reduction peak remains unchanged both at room and enhanced (60°C) temperatures. This means that radical cations $MV^{\bullet+}$ fail to reduce $[PtCl_4]^{2-}$ at a considerable rate.

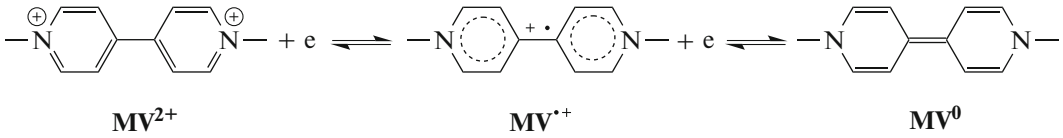

Scheme 2. Two-step reversible electroreduction of methylviologen.

It becomes evident that electrosynthesis of PtNPs via the methylviologen-mediated electroreduction of $[PtCl_4]^{2-}$ by the mechanism similar to that of the reduction of $[PdCl_4]^{2-}$ at the potentials of $MV^{\bullet+}$ generation is impossible. For the mediated process, one should use either the more efficient mediator or the easier reducible platinum substrate. From the standpoint of energy efficiency of the process, the latter version seems more attractive.

The reduction of $PtCl_2$ ($\Delta E_p \approx$ 1.0 V) proceeds much easier as compared with $[PtCl_4]^{2-}$ (Fig. 2) and in this case one should expect methylviologen to exhibit the mediator properties at the potentials of the $MV^{2+}/MV^{\bullet+}$ redox couple. This is why, this easily available substrate has been chosen here as the object of further studies. However, for this compound in DMSO, the peak of $[PtCl_4]^{2-}$ reduction is also observed. Insofar as $[PtCl_4]^{2-}$ is not reduced by meth-

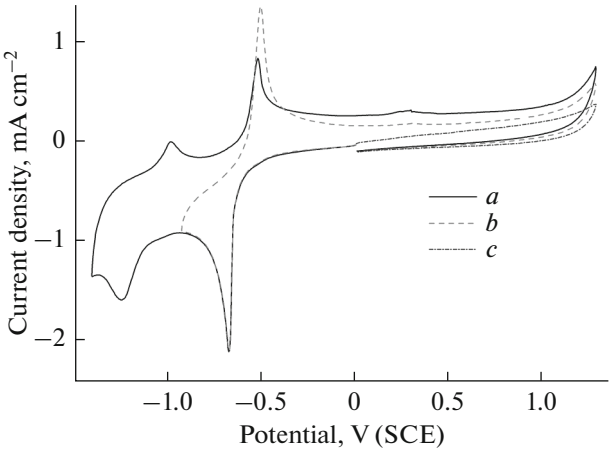

Fig. 3. CV curves of 2.0 mM MV^{2+} in H_2O/0.1 M KPF_6 with the initial potential scanning in the (*a, b*) cathodic and (*c*) anodic direction. Reversal potential: (*a*) −1.40 V and (*b*) −0.93 V. v = 100 mV/s.

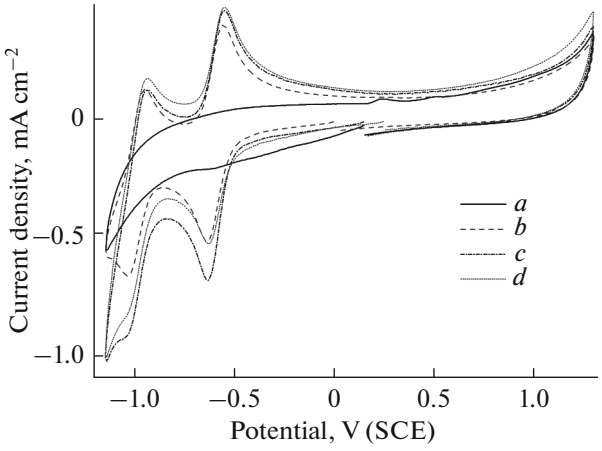

Fig. 4. CV curves of (*a*) 1.5 mM $PtCl_2$, (*b*) 2.0 mM MV^{2+}, and (*c, d*) the system of 2.0 mM MV^{2+} + 1.5 mM $PtCl_2$ (*c*) before and (*d*) after electrolysis at −0.80 V (Q = 2.0 F per $PtCl_2$) in the DMF (40 vol %)–H_2O/0.1 M KPF_6 medium. v = 100 mV/s.

ylviologen mediation, one can hardly expect a priory the quantitative electroreduction of $PtCl_2$ at the mediated electrosynthesis in this medium. The solvation energy of ions increases with the increase in the dielectric permittivity of the medium and the decrease in the ion radius. Hence, generally, as the medium polarity increases, one should expect the increase in the degree of dissociation of $[PtCl_4]^{2-}$ and also in the mobility of equilibrium between $[PtCl_4]^{2-}$ and $PtCl_2$ (Scheme 1). Correspondingly, when we pass from DMSO (ε = 37) to water (ε = 78) and to water-organic media with the minimum content of the organic component, one can also expect the partial or total reduction of generated $[PtCl_4]^{2-}$ due to the shift of equilibrium according to the Le Chatelier principle and, as a consequence, the increase in the yield of PtNPs.

The necessary condition for the efficient mediated electrosynthesis of MNPs in the solution bulk is also the absence of adsorption on the electrode both for the mediator and its reduced form. In the aqueous medium, the $MV^{2+} \cdot 2PF_6^-$ salt is adsorbed on the electrode, as follows from the adsorption nature of its first reduction peak (Fig. 3, curves *a*, *b*). The minimum content of DMF for which this salt is not adsorbed is 40 vol %. In this medium, both peaks of methylviologen reduction to cation radical $MV^{\bullet+}$ and neutral diamine MV^0 are perfectly reversible (Fig. 4b). The totality of factors discussed above necessitate the choice of this medium as the basic one for the more detailed study.

In the DMF (40 vol %) – H_2O/0.1 M KPF_6 medium, $PtCl_2$ is not dissolved in considerable amount so that for its calculated concentration of 1.5 mM, its main part resides as the precipitate. Hence, the CV curve shows no clear peaks of its reduction, demonstrating only a continuous increase in the current throughout the whole accessible range of cathodic potentials (Fig. 4a). The CV curve of the mixture of $PtCl_2$ (1.5 mM) with MV^{2+} (2.0 mM) represents the summarized curves of individual components (Fig. 4c). The CV data (i) neither reject nor confirm the presence of mediated reduction of $PtCl_2$; (ii) make it possible to choose the potential for the preparative mediated electrolysis to generate methylviologen radical cations (−0.80 V vs. SCE); (iii) indicate that at this potential, the reduction of $PtCl_2$ immediately on the electrode proceeds with the much lower rate as compared with the mediator reduction.

Electrosynthesis of Platinum Nanoparticles in the Absence of Stabilizer

For the preparative reduction of a solution containing 1.5 mM $PtCl_2$, 2.0 mM $MV^{2+} \cdot 2PF_6^-$ at the controlled potential of mediator reduction (−0.80 V), the current in the course of electrolysis (~30 min) gradually decreases ($I \approx 3.6 \rightarrow 1.3$ mA). The original turbid light-yellow solution (Fig. 5a) acquires the light-blue color typical of methylviologen radical cations (Fig. 5b) from the very first seconds of electrolysis. This color is retained during the whole period of electrolysis. At a certain time after the end of electrolysis (~5 min), the blue color disappears and the solution becomes dark grey, which is associated with the presence of black suspension (Fig. 5c). The CV curve of the resulting solution demonstrates only the peaks of reduction and reoxidation of methylviologen, totally resembling the curve of individual methylviologen of the same concentration (Fig. 4). This means that

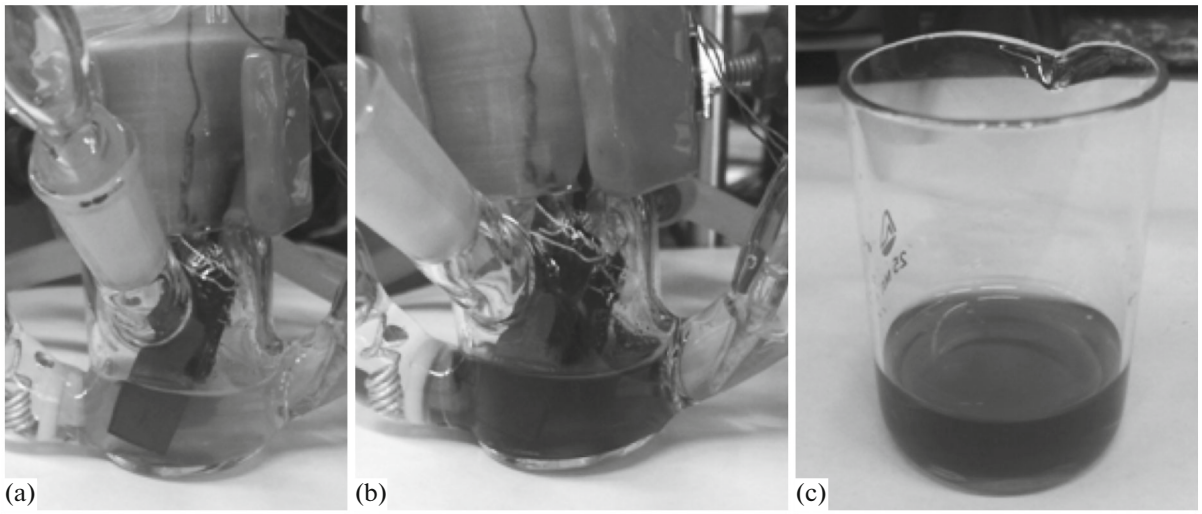

Fig. 5. Photographs of the solution of $PtCl_2$ (1.5 mM) + MV^{2+} (2.0 mM) in DMF (40 vol %)–H_2O/0.1 M KPF_6 collected (a) before, (b) during, and (c) after the electrolysis at –0.80 V (Q = 2.0 F per $PtCl_2$).

methylviologen is not consumed during the electrolysis, although the electrolysis occurs at the potentials of its reduction to radical cation. In is probable that a sufficiently slow process of mediated electroreduction of $PtCl_2$ to form metal platinum particles takes place (Scheme 3). A small part (14%) of metal is deposited on the cathode as evidenced by the gain in the electrode mass during the electrolysis (0.4 mg). Its main part (86%) remains in solution as black precipitate.

$$2n\mathrm{MV}^{2+} + 2n\mathrm{e} \rightleftharpoons 2n\mathrm{MV}^{\bullet+}$$
$$2n\mathrm{MV}^{\bullet+} + n\mathrm{PtCl}_2 \rightarrow \left(\mathrm{Pt}^0\right)_n + 2n\mathrm{MV}^{2+} + 2n\mathrm{Cl}^-$$

Scheme 3. Methylviologen mediated reduction of $PtCl_2$.

In the solution obtained by dispersing the synthesized NPs to water (see Experimental), the DLS studies revealed sufficiently coarse particles with the average hydrodynamic diameter of 270 and 945 nm (Fig. 6a). At the same time, the majority of particles had the average size of 238 and 873 nm. According to results of SEM (Fig. 6b) and TEM (Figs. 6c, 6d) studies, the NPs were of diverse shape and coalesced to form various aggregates, including those shaped as "snowflakes". Their energy-dispersive spectrum (Fig. 6e) confirms the presence of platinum in them.

The MNPs are thermodynamically unstable because of the uncompensated valence of surface atoms; hence, their aggregation (agglomeration) and adsorption on hydrophobic surfaces in the absence of NPs stabilizers are common. This is why, it seems sufficiently reasonable that PtNPs aggregates are formed and a part of metal generated by mediated synthesis in the solution bulk is deposited on the surface of the glassy-carbon electrode. At the same time, in this case, the metal deposition on the electrode may the associated with another factor. The point is that at the electrolysis potential, the deposition of not only the mediator but also of $PtCl_2$ can occur at a low rate (Fig. 4). Insofar as radical cations $MV^{\bullet+}$ reduce $PtCl_2$ very slowly, the "protective layer" of $MV^{\bullet+}$ in the near-electrode layer probably fails to "catch" and reduce all $PtCl_2$ species arriving from solution. Thus, one cannot rule out the possibility of partial reduction of $PtCl_2$ on the electrode and the deposition of generated metal.

Electrosynthesis of Platinum Nanoparticles in the Presence of Silica Nanoparticles

The CV curves of the solution containing 2 mM $MV^{2+} \cdot 2PF_6^-$, 1.5 mM $PtCl_2$, 2 g/L SiO_2 show no clear peaks of $PtCl_2$ reduction, demonstrating only the peaks of methylviologen reduction and reoxidation (Fig. 7). The reduction peaks are somewhat higher and the reoxidation peaks are somewhat lower than the corresponding peaks in the absence of $PtCl_2$, which may be a result of the mediated reduction of $PtCl_2$. In the preparative reduction of this solution at the potential fixed at –0.80 V, the current during the electrolysis (38 min) smoothly decays ($I \approx 2.2 \rightarrow 1.1$ mA). Visually, the same changes as in the absence of SiO_2 are observed during and after the electrolysis. In the CV curve measured in the electrolyzed solution, only the peaks of methylviologene reduction and reoxidation can be seen, which corresponds completely to the curve of individual methylviologen with the same concentration. The mass of the working electrode after the electrolysis increased by 0.4 mg. Obviously, the presence of SiO_2 NPs in solution has no effect on the mediated reduction of $PtCl_2$: metylviologen is not consumed during the electrolysis, sufficiently slow

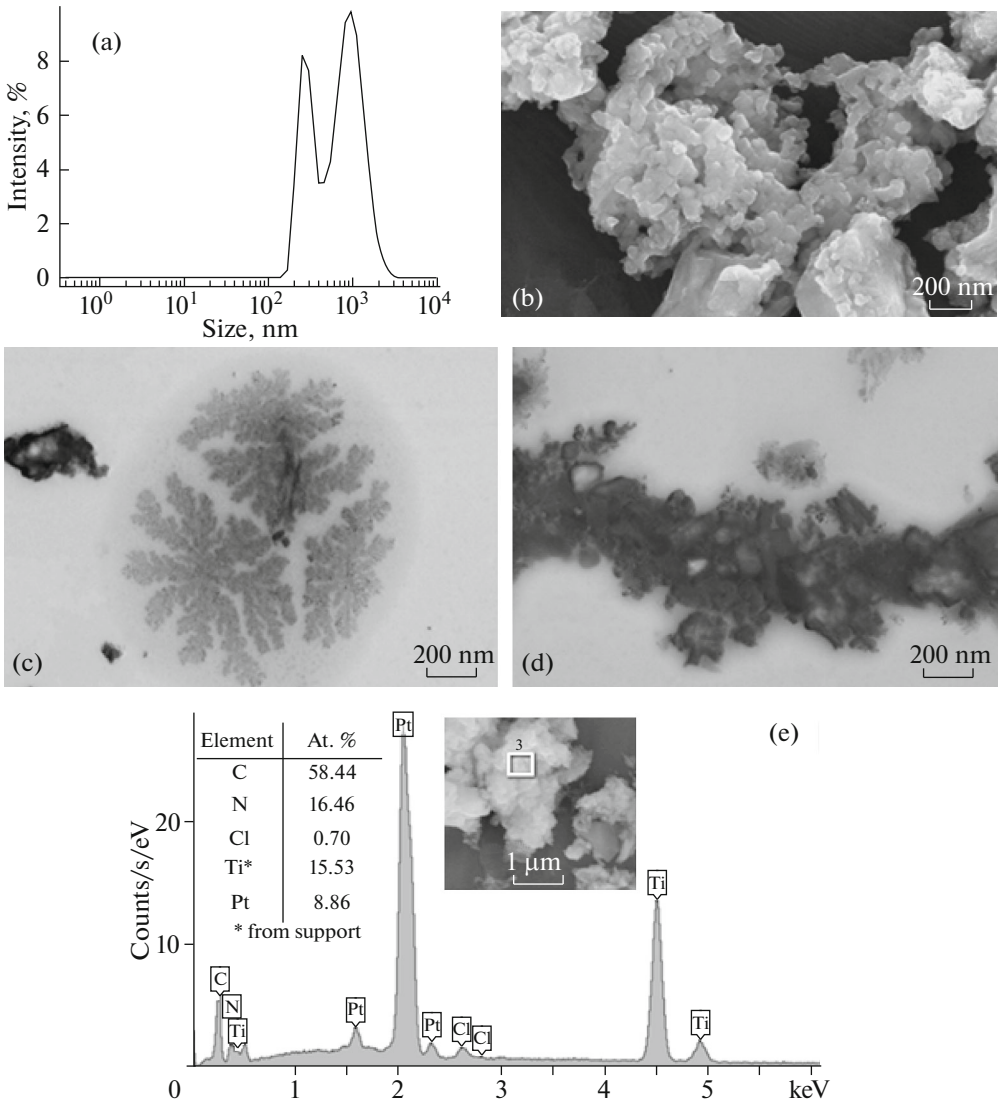

Fig. 6. (a) Diagram of size distribution (DLS, PdI = 0.521 ± 0.007); (b) SEM and (c, d) STEM images, and (d) energy-dispersive spectrum for PtNPs. Insert (d), the square marks the site where the energy-dispersive spectrum was collected.

mediated electroreduction of $PtCl_2$ to form metal platinum particles takes place (Scheme 3), 14% of generated metal is deposited on the electrode, while 86% stays in solution.

In the SEM (Fig. 8a) and TEM (Fig. 8b) images of NPs extracted from the solution by centrifugation, spherical NPs of the size (86 ± 25 nm) the same as SiO_2 particles can be seen, as well as other particles of various size and shape. According to energy-dispersive spectrum (Fig. 8c), the latter represent PtNPs. The map of element distribution shows that spherical NPs contain Si, O, C and virtually no platinum (Fig. 9), i.e., similarly to the methylviologen-mediated electrosynthesis of PdNPs [26], the generated PtNPs are neither immobilized nor stabilized to any considerable extent on the hydrophobic surface of silica NP. In the presence of SiO_2 NPs, they behave in the same manner as in their absence, aggregate and form coarser particle of various size and shape.

Thus, these results suggest that SiO_2 NPs are involved neither in the mediated reduction of $PtCl_2$ nor in stabilization of PtNPs formed.

Electrosynthesis of Platinum Nanoparticles in the Presence of SiO_2-NHR Nanoparticles

In the presence of NP SiO_2-NHR (1 g/L), in the CV curves of the solution containing 2 mM $MV^{2+} \cdot 2PF_6^-$, 1.5 mM $PtCl_2$ recorded prior (Fig. 7) and after the electrolysis, the phenomena observed during the electrolysis at the potential fixed at −0.80 V are totally analogous to those observed in the presence of SiO_2. Virtually the same amount of metal (0.5 mg) is depos-

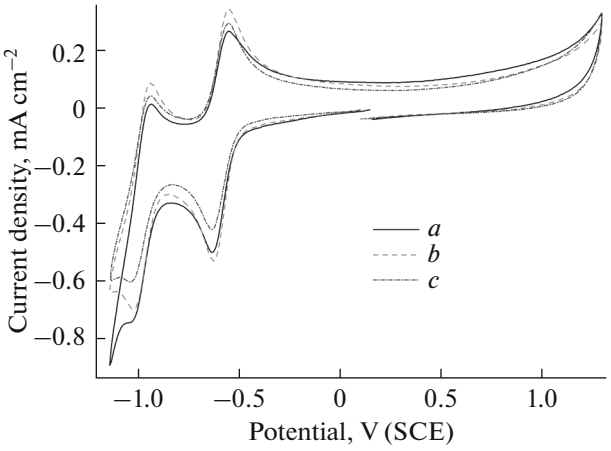

Fig. 7. CV curves of the system 2 mM MV^{2+} + 1.5 mM $PtCl_2$ in the presence of (*a*) 2 g/L SiO_2, (*b*) 1 g/L SiO_2-NHR, and (*c*) 8.3 g/L PVP in the DMF (40 vol %)–H_2O/0.1 M KPF_6 medium. v = 100 mV/s.

ited on the working electrode. Evidently, the presence of SiO_2-NHR nanoparticles in solution also has no effect on the mediated reduction of $PtCl_2$: in this case, methylviologen is not consumed during the electrolysis and the sufficiently slow mediated electroreduction of $PtCl_2$ proceeds to form metal platinum particles (Scheme 3) of which 18% forms the metal deposit on the electrode and 82% stays in solution.

SEM (Fig. 10a) and TEM (Fig. 10b) images of the NPs extracted from the electrolyzed solution by centrifugation demonstrate spherical SiO_2-NHR NPs of the same size (157 ± 40 nm) as individual particles as well as other particles of different size and shape. According to the energy-dispersive spectrum (Fig. 10c), the latter particles are PtNPs. The map of element distribution (Fig. 11) shows that SiO_2-NHR NPs contain small amounts of Pt in addition to Si, O, C. Hence, as in the case of methylviologen-mediated electrosynthesis of NPs of Pd [24], Ag [31], Au [34], the generated PtNPs are partly immobilized and stabilized on the surface of silica NPs modified by alkylamine groups. Apparently, it is the alkylamine groups that bind the untrafine PtNPs (3 ± 2 nm) in the SiO_2-NHR surface layer (Fig. 10b).

Thus, SiO_2-NHR NPs, like SiO_2 NPs, are uninvolved in the mediated reduction of $PtCl_2$ but, in con-

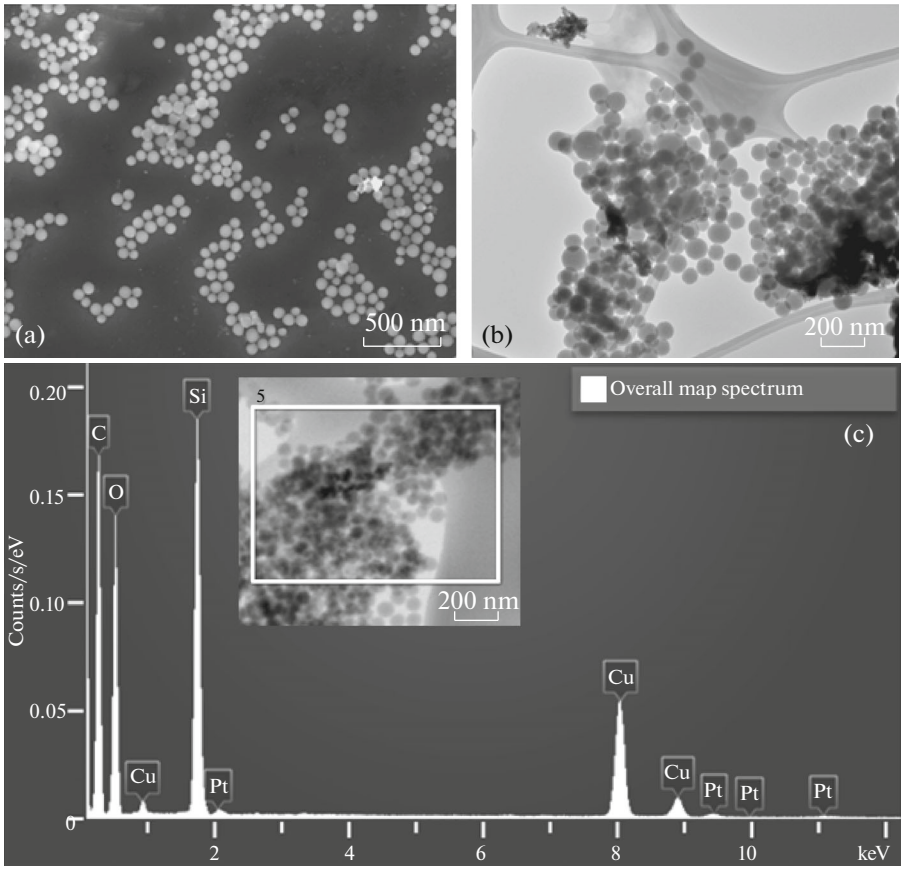

Fig. 8. (a) SEM and (b) TEM images and (c) energy-dispersive spectrum of Pt-SiO_2 nanoparticles. Insert (c): the square indicates the site where the energy-dispersive spectrum was collected.

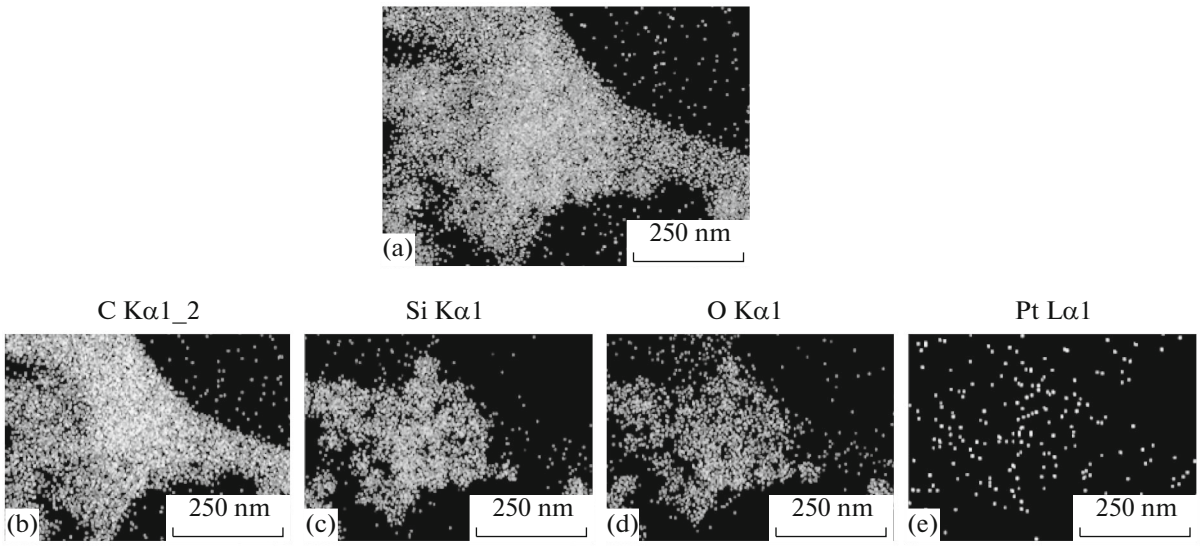

Fig. 9. Map of distribution of elements in Pt-SiO_2 nanoparticles: (a) multilayer map, (b) carbon, (c) silicon, (d) oxygen, (e) platinum.

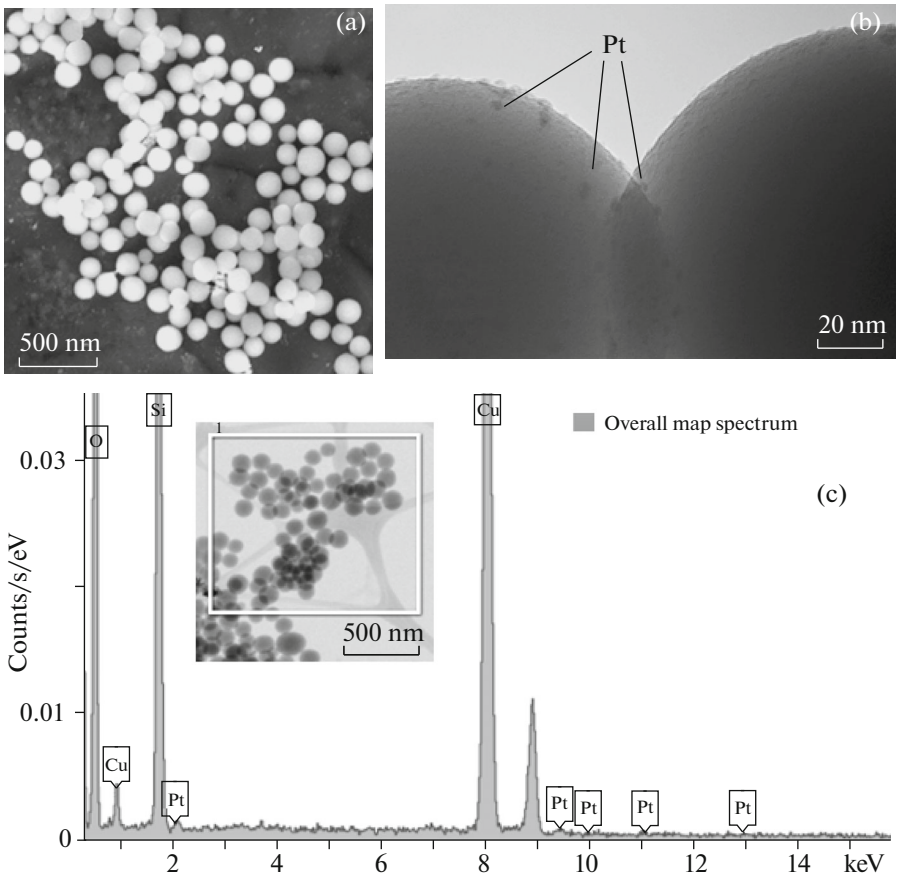

Fig. 10. (a) SEM and (b) TEM images and (c) energy-dispersive spectrum of Pt-SiO_2-NHR nanoparticles. Insert (c): the square marks the site where the energy-dispersive spectrum was collected.

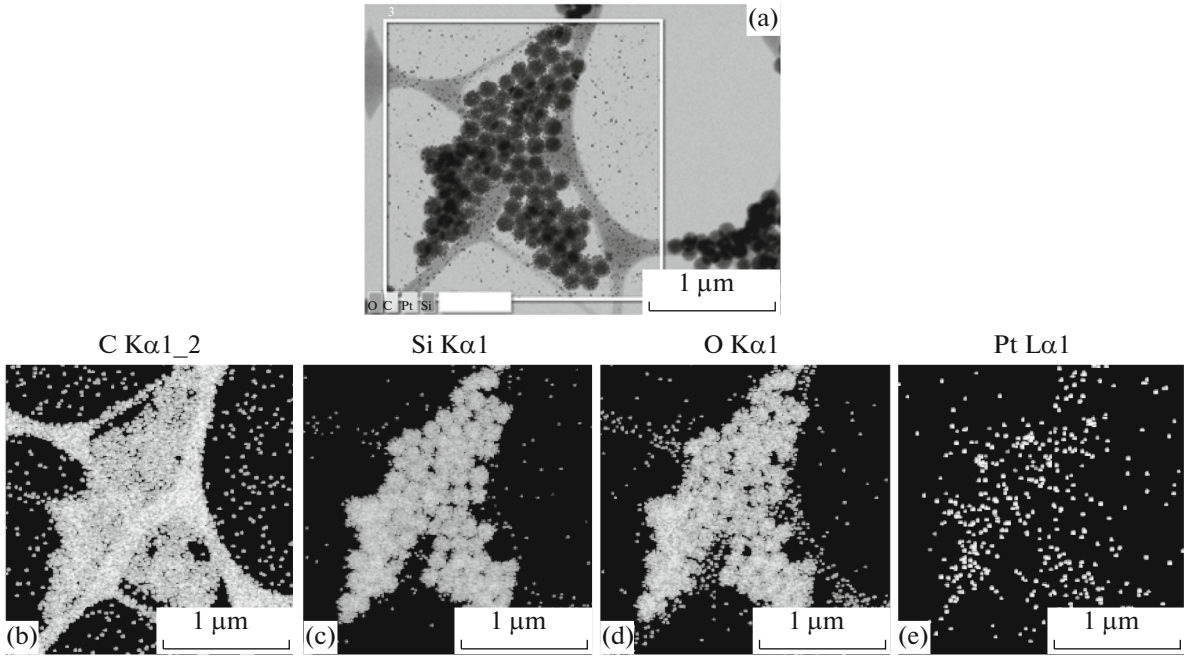

Fig. 11. Map of distribution of elements in Pt-SiO_2-NHR nanoparticles in the marked region: (a) multilayer map (b) carbon, (c) silicon, (d) oxygen, (e) platinum.

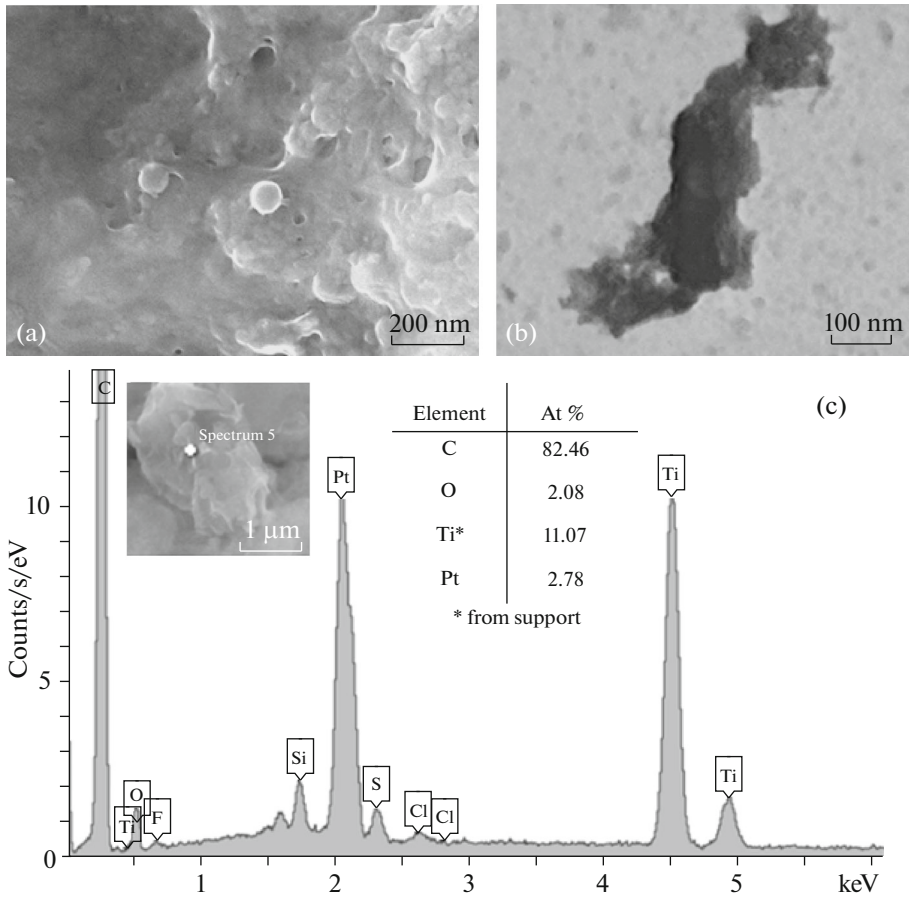

Fig. 12. (a) SEM and (b) STEM images and (c) energy-dispersive spectrum of PVP-stabilized PtNPs deposited from solution 1. Insert (c): the cross marks the site where the energy-dispersive spectrum was collected.

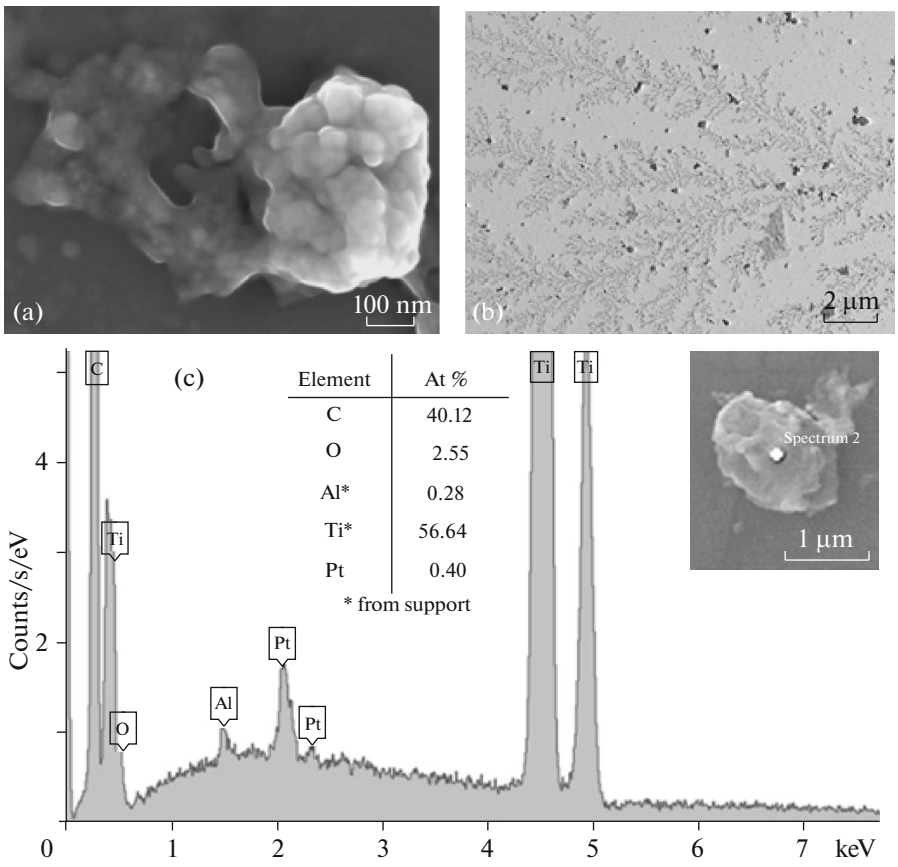

Fig. 13. (a) SEM and (b) STEM images and (c) energy-dispersive spectrum of PVP-stabilized PtNPs deposited from 10-times diluted solution 1. Insert (c): the cross marks the site where the energy-dispersive spectrum was collected.

trast, partly bind and stabilize the formed PtNPs in their surface layer.

Electrosynthesis of Platinum Nanoparticles in the Presence of Polyvinylpyrrolidone

As in the previous examples, the introduction of 8.3 g/L PVP to solution containing 2 mM $MV^{2+} \cdot 2PF_6^-$, 1.5 mM $PtCl_2$ has no effect on the morphology of the CV curves recorded before (Fig. 7) and after the electrolysis and also on the preparative electrolysis carried out at the potential fixed at –0.80 V. The effect of PVP is manifested, however, in the results of electrolysis. In contrast to the above electrolyses, the dark-brown solution obtained in this electrolysis is homogeneous and the mass of the working electrode remains unchanged during the electrolysis. It is evident that in this case we observe the methylviologen-mediated electroreduction of $PtCl_2$ to form NPs of metal platinum (Scheme 3). In this case, the generated metal is bound and stabilized by PVP and hence, is not deposited on the electrode, remaining totally in solution.

Centrifugation (15000 rpm, 2 h) of this solution failed to precipitate NPs. This is why, the solvent was distilled away from solution under reduced pressure. A part of resulting precipitate was dispersed to water, the NPs were precipitated by centrifugation, washed three times with twice distilled water, and dispersed in water (solution 1). The other part of precipitate was cleaned from the supporting electrolyte by dialysis. For this purpose, the precipitate was dissolved in 4 mL of water and placed into the dialysis sac with pores that let pass through the particles with the mass below 1000 D. The sac was placed in 1 L of twice distilled water stirred with magnetic stirrer. Water was changed twice. The sac was kept in water for 1 h in the first step, 2 h in the second step, and 3 h in the third step. Ultimately, we obtained solution 2.

In the SEM image of particles in solution 1 (Fig. 12a), individual NPs are virtually absent, they form a sort of formless common mass. According to energy-dispersive spectrum (Fig. 12c) and STEM data (Fig. 12b), this mass contains mainly PVP with inclusions of PtNPs (~18 ± 9 nm). It is obvious that PVP polymer molecules not only stabilize PtNPs by encapsulating the latter but also are bound with one another to form the common mass. When solution 1 is diluted 10-fold, the common mass still forms, but NPs are manifested more clearly and the STEM images reveal

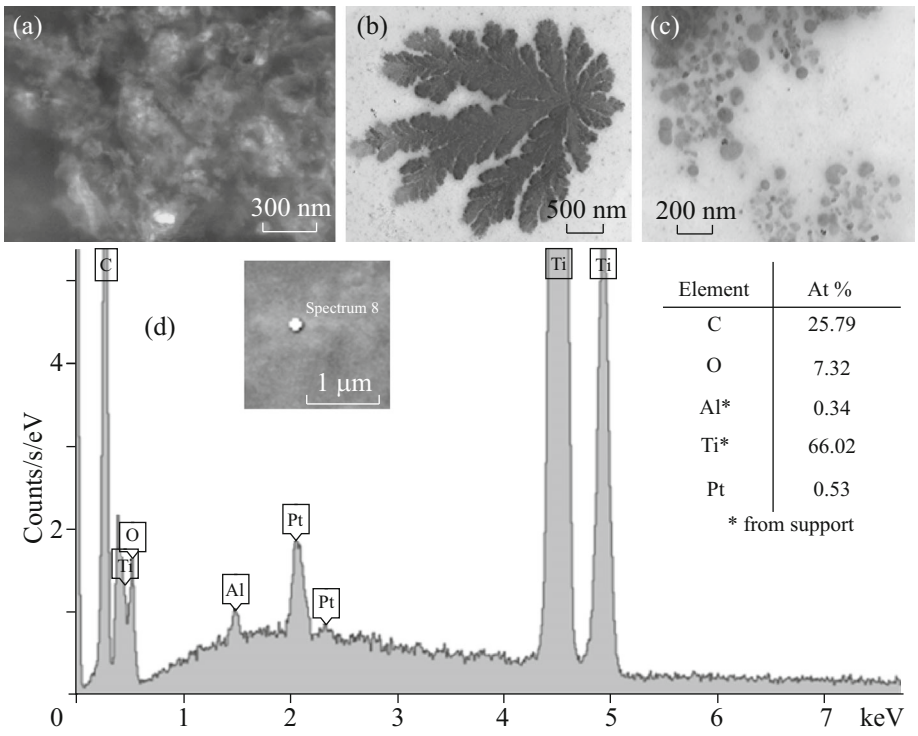

Fig. 14. (a) SEM and (b, c) STEM images and (d) energy-dispersive spectrum of PVP-stabilized PtNPs deposited from solution 2. Insert (d): the cross marks the site where the energy-dispersive spectrum was collected.

in addition to individual PtNPs, their aggregates such as "snowflakes" (Fig. 13b). The similar behavior is typical also of particles in solution 2; however, in this case the coarser spherical NPs are observed too (Fig. 14).

CONCLUSIONS

Pursuing our earlier investigations on the mediated electrosynthesis of metal nanopartincles in solution volume [23–35], we electrosynthesized platinum nanoparticles by methylviologen-mediated reduction of $PtCl_2$ at the potentials of the $MV^{2+}/MV^{\bullet+}$ redox couple in 40% aqueous DMF (Scheme 3). In contrast to $[PdCl_4]^{2-}$ [23–28], Ag^+ [29, 30], AgCl [31, 32], AuCl [34], the methylviologen radical cation reduces $PtCl_2$ much more slowly. In the absence of stabilizers of nanoparticles, 14% of generated PtNPs is deposited on the electrode, while 86% remains in solutions as coarse aggregates which form the precipitate. When PtNPs are deposited on a formvar/carbon support, individual PtNPs and their aggregates in the form of "snowfakes" can be observed. The surface of spherical silicate nanoparticles (86 ± 25 nm) is covered with hydrophilic Si-OH groups which can bind neither $PtCl_2$, nor MV^{2+}, nor generated PtNPs. Hence, their introduction to solution has no effect on the mediated reduction of $PtCl_2$ and the results of mediated electrosynthesis. The surface layer of alkylamine-modified silica NPs SiO_2-NHR (157 ± 40 nm) contains amino groups and hydrophilic alkyl fragments, which are potentially capable of binding PtNPs via coordination and hydrophobic interactions. Hence, at the electrolysis in the presence of SiO_2-NHR NPs, the generated PtNPs, besides being deposited on the electrode (18%) and forming coarse aggregates in solution, are partly bound to form individual ultrafine NPs (3 ± 2 nm) on the surface of SiO_2-NHR. In the presence of PVP, the generated PtNPs (18 ± 9 nm) neither aggregate nor deposit on the cathode but are completely stabilized in solution being encapsulated in the PVP matrix. Being deposited onto support of titanium or formvar/carbon, they form the common aggregate because the PVP polymer molecules are bound to one another. In the latter case, under certain conditions, individual PtNPs and their "snowflake" aggregates can be observed. The resulting platinum nanoparticles were characterized by the methods of dynamic light scattering and scanning, transmission, and scanning transmission electron microscopy.

ACKNOWLEDGMENTS

This study was financially supported by the Russian Foundation for Basic Research (grant 14-03-00405).

REFERENCES

1. Pomogailo, A.D., Rozenberg, A.S., and Uflyand, I.E., *Nanochastitsy metallov v polimerakh (Metal Nanoparticles in Polymers)*, Moscow: Khimiya, 2000.
2. Roldugin, V.I., *Russ. Chem. Rev.*, 2000, vol. 69, p. 821.
3. Daniel, M.C. and Astruc, D., *Chem. Rev.,* 2004, vol. 104, p. 293.
4. Suzdalev, I.P., *Nanotekhnologiya: Fiziko-khimiya nanoklasterov, nanostruktur i nanomaterialov (Nanotechnology: Physical Chemistry of Nanoclusters, Nanostructures, and Nanomaterials)*, Moscow: Librokom, 2009, 2nd Ed.
5. Volkov, V.V., Kravchenko, T.A., and Roldugin, V.I., *Russ. Chem. Rev.*, 2013, vol. 82, p. 465.
6. Dykman, L.A., Bogatyrev, V.A., Shchegolev, S.Yu., and Khlebtsov, N.G., in *Zolotye nanochastitsy. Sintez, svoistva, biomeditsinskoe primenenie (Gold Nanoparticles: Synthesis, Properties, and Biomedicinal Application)*, Moscow: Nauka, 2008.
7. *Handbook of Less-Common Nanostructures*, Kharisov, B.I., Kharissova, O.V., and Ortiz-Méndez, U., Eds., Boca Raton: CRC, 2012.
8. Faraday, M., *Philos. Trans. Roy. Soc. London,* 1857, vol. 147, p. 145.
9. Egorova, E.M., *Nanotekhnika,* 2004, p. 15.
10. Egorova, E.M., *Russ. J. Phys. Chem. A,* 2010, vol. 84, p. 629.
11. Petrii, O.A., *Russ. Chem. Rev.,* 2015, vol. 84, p. 159.
12. Haber, F., *Z. Anorg. Chem.,* 1898, vol. 16, p. 438.
13. Rodrigues-Sanchez, L., Blanko, M.L., and Lopez-Quintela, M.A., *J. Phys. Chem. B*, 2000, vol. 104, p. 9683.
14. Yin, B., Ma, H., Wang, S., and Chen, S., *J. Phys. Chem. B,* 2003, vol. 107, p. 8898.
15. Saez, V. and Mason, T.J., *Molecules,* 2009, vol. 14, p. 4284.
16. Zhu, J., Liu, S., Palchik, O., Koltypin, Y., and Gedanken, A., *Langmuir,* 2000, vol. 16, p. 6396.
17. Reisse, J., Caulier, T., Deckerkheer, C., Fabre, O., Vandercammen, J., Delplancke, J.L., and Winand, R., *Ultrason. Sonochem.,* 1996, vol. 3, p. 147.
18. Reetz, M.T. and Helbig, W., *J. Am. Chem. Soc.,* 1994, vol. 116, p. 7401.
19. Becker, J.A., Schäfer, R., Festag, R., Ruland, W., Wendorff, J.H., Pebler, J., Quaiser, S.A., Helbig, W., and Reetz, M.T., *J. Chem. Phys.,* 1995, vol. 103, p. 2520.
20. Reetz, M.T., Quaiser, S.A., and Merk, C., *Chem. Ber.,* 1996, vol. 129, p. 741.
21. Reetz, MT., Helbig, W., Quaiser, S.A., Stimming, U., Breuer, N., and Vogel, R., *Science,* 1995, vol. 267, p. 367.
22. Reetz, M.T., Winter, M., Breinbauer, R., Thurn-Albrecht, T., and Vogel, W., *Chem. - Eur. J.,* 2001, vol. 7, p. 1084.
23. Yanilkin, V.V., Nasybullina, G.R., Ziganshina, A.Yu., Nizamiev, I.R., Kadirov, M.K., Korshin, D.E., and Konovalov, A.I. *Mendeleev Commun.*, 2014, vol. 24, p. 108.
24. Yanilkin, V.V., Nasybullina, G.R., Sultanova, E.D., Ziganshina, A.Yu., and Konovalov, A.I., *Russ. Chem. Bull.,* 2014, vol. 63, no. 6, p. 1409.
25. Yanilkin, V.V., Nastapova, N.V., Nasretdinova, G.R., Mukhitova, R.K., Ziganshina, A.Yu., Nizameev, I.R., and Kadirov, M.K., *Russ. J. Electrochem.,* 2015, vol. 51, p. 951.
26. Fedorenko, S., Jilkin, M., Nastapova, N., Yanilkin, V., Bochkova, O., Buriliov, V., Nizameev, I., Nasretdinova, G., Kadirov, M., Mustafina, A., and Budnikova, Y., *Colloids Surf., A,* 2015, vol. 486, p. 185.
27. Yanilkin, V.V., Nastapova, N.V., Sultanova, E.D., Nasretdinova, G.R., Mukhitova, R.K., Ziganshina, A.Yu., Nizameev, I.R., and Kadirov, M.K., *Russ. Chem. Bull.,* 2016, vol. 65, p. 125.
28. Nasretdinova, G.R., Osin, Y.N., Gubaidullin, A.T., and Yanilkin, V.V., *J. Electrochem. Soc.,* 2016, vol. 163, p. G99.
29. Nasretdinova, G.R., Fazleeva, R.R., Mukhitova, R.K., Nizameev, I.R., Kadirov, M.K., Ziganshina, A.Yu., and Yanilkin, V.V., *Electrochem. Commun.,* 2015, vol. 50, p. 69.
30. Nasretdinova, G.R., Fazleeva, R.R., Mukhitova, R.K., Nizameev, I.R., Kadirov, M.K., Ziganshina, A.Yu., and Yanilkin, V.V., *Russ. J. Electrochem.,* 2015, vol. 51, p. 1029.
31. Yanilkin, V.V., Nastapova, N.V., Nasretdinova, G.R., Fazleeva, R.R., and Osin, Y.N., *Electrochem. Commun.,* 2015, vol. 59, p. 60.
32. Nasretdinova, G.R., Fazleeva, R.R., Osin, Y.N., Gubaydullin, A.T., and Yanilkin, V.V., *Russ. J. Electrochem.,* 2017, vol. 53.
33. Yanilkin, V.V., Nasretdinova, G.R., Osin, Y.N., and Salnikov, V.V., *Electrochim. Acta,* 2015, vol. 168, p. 82.
34. Yanilkin, V.V., Nastapova, N.V., Nasretdinova, G.R., Fedorenko, S.V., Jilkin, M., Mustafina, A.R., Gubaidullin, A.T., and Osin, Y.N., *RSC Adv.,* 2016, vol. 6, p. 1851.
35. Yanilkin, V.V., Nastapova, N.V., Nasretdinova, G.R., Fazleeva, R.R., and Osin, Y.N., *Electrochem. Commun.,* 2016, vol. 69, p. 36.
36. Leontyev, I., Kuriganova, A., Kudryavtsev, Y., Dkhil, B., and Smirnova, N., *Appl. Catal., A,* 2012, vol. 431–432, p. 120.
37. Weitz, E., *Angew. Chem.,* 1954, vol. 66, p. 658.

Translated by T. Safonova